Controllable Self-Assembly

Deutsche Ausgabe: DOI: 10.1002/ange.201509071
Internationale Ausgabe: DOI: 10.1002/anie.201509071

Dual-Mode Controlled Self-Assembly of TiO_2 Nanoparticles Through a Cucurbit[8]uril-Enhanced Radical Cation Dimerization Interaction

Qi Zhang, Da-Hui Qu, Qiao-Chun Wang, and He Tian**

Abstract: *The realization of controllable multicomponent self-assembly through reversible supramolecular interactions is a challenging goal, and is an important strategy for the fabrication of switchable nanomaterials. Herein we show that the self-assembly of TiO_2 nanoparticles (NP) functionalized with methyl viologen can be controlled both by light irradiation and chemical reduction through cucurbit[8]uril-enhanced radical cation dimerization interactions. Moreover, the controlled assembly and disassembly of this system are accompanied by switchable photocatalytic activity of the TiO_2 NPs, which shows potential application as a novel smart and recyclable photocatalyst.*

Supramolecular systems, especially host–guest systems operating on surfaces or interfaces, have attracted much attention because of their practical applications.[1,2] One particularly interesting field involved the utilization of supramolecular interactions as the "glue" for the assembly of nanoparticles (NPs) in a precisely controllable manner through one or more external stimuli.[3] The assembled NP systems had a number of unexpected and interesting properties,[4] for example in terms of their optical properties,[4a] morphology,[4b] aggregation,[4c] spectroscopy,[4d] and catalytic activity,[4e] making them suitable candidates for the construction of switchable hybrid nanomaterials. The multi-stimuli-responsive self-assembly of NPs is more promising because it can provide a versatile means to "encode" the NPs.[5] For example, Klajn and co-workers reported intriguing dual-stimuli-responsive azobenzene-functionalized Fe_3O_4 NPs[5b] and gold NPs,[5d] respectively, which showed great potential in controlled self-assembly and in the development of logic gates.

Radical cation dimerization is widely used in traditional organic synthesis. It has been demonstrated that radical cation dimerization can be stabilized by threading through the cavity of macrocyclic hosts to form stable supramolecular host–guest complexes,[6] providing a new template for the construction of mechanically interlocked molecules.[7] However, to our knowledge, radical cation dimerization interactions have been rarely employed to bind TiO_2 NPs together.[4h] Herein we report, for the first time, the dual-mode precise control of the self-assembly of TiO_2 NPs through a cucurbit[8]uril-enhanced radical cation dimerization interaction (Figure 1). In this system, the redox-active methyl viologen dication (MV^{2+}) groups were covalently attached onto TiO_2 NPs. The MV^{2+} ion can then be reduced to form the $MV^{+\bullet}$ radical cation by chemical reduction, leading to the typical dimerization of $MV^{+\bullet}$ units in the cavity of cucurbit[8]uril (CB[8]), followed by aggregation of the TiO_2 NPs. Alternatively, the assembly of TiO_2 NPs can be realized photochemically. Employing this method, the TiO_2 NPs act as a photosensitizer to reduce the MV^{2+} dication into the $MV^{+\bullet}$ radical cation in response to a light stimulus in aqueous solution.[8] It should be noted that this system is reversible and can be employed as a switchable and recyclable water-soluble photocatalyst. As a result of the ability of TiO_2 NPs to produce oxidizing radicals in biological environments and their activity in photocatalytic reactions,[9] this novel hybrid system may have potential applications in biological fields and in photocatalytic organic synthesis.

In order to bind MV^{2+} groups onto the surface of the TiO_2 NPs, a typical enediol ligand was selected as the covalent linker. This ligand has shown a greater affinity for TiO_2

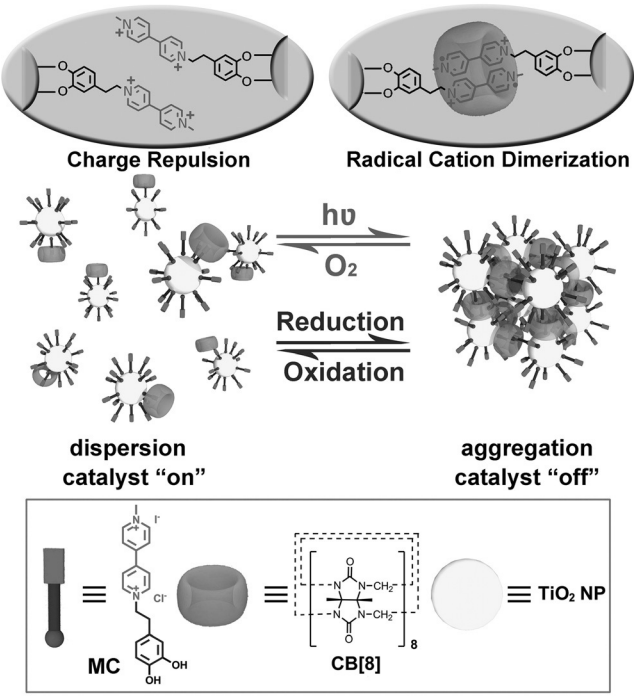

Figure 1. Schematic representation of the self-assembly of MV^{2+}–TiO_2 NPs through photochemical and chemical-reduction modes, respectively.

[*] Q. Zhang, Prof. D.-H. Qu, Prof. Q.-C. Wang, Prof. H. Tian
Key Laboratory for Advanced Materials and Institute of Fine Chemicals, East China University of Science and Technology
130 Meilong Road, Shanghai, 200237 (China)
E-mail: dahui_qu@ecust.edu.cn
tianhe@ecust.edu.cn

Supporting information for this article is available on the WWW under http://dx.doi.org/10.1002/anie.201509071.

because of its strong coordinative interaction with unsaturated Ti^{IV} atoms on the surface of the TiO_2 NPs.[10] Treatment of catechol-terminated methyl viologen MC (Figure 1; Figure S1–S4 in the Supporting Information) with $TiCl_4$ produced MV^{2+}–TiO_2 NPs by using a modified version of a reported procedure (Figure S5).[10a] X-ray diffraction (XRD), X-ray photoelectron spectroscopy (XPS), and high-resolution transmission electron microscopy (HR-TEM) were used to confirm the successful hybridization of MC and TiO_2. First, the XRD pattern (Figure S6) showed the typical anatase-phase diffraction peaks of TiO_2 (JCPDS card no. 21-1272) with high crystallinity as a result of the sharp peaks distributed to (101), (004), and (200) lattice planes. The electron diffraction patterns and clear lattice fringes detected by HR-TEM and selected area electron diffraction (SAED) also confirmed the results obtained by XRD (Figure S7). The high crystallinity of the material, a result of the efficient synthetic process and a long aging time, also indicated high photoactivity.[11] The coverage of ligand MC on the surface of the TiO_2 NPs was calculated using cyclic voltammetry to be approximately $(8.37 \pm 0.01) \times 10^{-12}$ mol cm^{-2} (Figure S8).[12] XPS spectra were used to detect the covalent link between MV^{2+}–enediol and the Ti atoms on the TiO_2 surface. The high-energy-resolution O 1s core level spectrum is shown in Figure S9c. In this spectrum, the asymmetric O 1s profile can be fit to two symmetrical peaks located at 530.5 eV and 532.0 eV, indicating that there are two types of O species on the surface of the MV^{2+}–TiO_2 NPs: the lattice oxygen of TiO_2 and the oxygen of MC coordinated to Ti atoms.[10d] Thus, it was demonstrated that the MV^{2+} moieties were successfully linked to the surface of TiO_2 NPs by covalent bonds.

We then focused on the controllable self-assembly of MV^{2+}–TiO_2 NPs in response to chemical and photochemical stimuli. First, an aqueous solution of MV^{2+}–TiO_2 NPs was preassembled with CB[8] to give a transparent yellow solution. After addition of excess $Na_2S_2O_4$, the transparent yellow solution became opaque and turned dark blue quickly, a characteristic color of the complex $2(MV^{+\bullet})$@CB[8], indicating that radical cation dimerization had occurred in the cavity of CB[8]. A dark-gray precipitate was obtained five minutes after the addition of $Na_2S_2O_4$ (Figure S10), which can be attributed to the aggregation of TiO_2 NPs (having low solubility) instead of intra-particle dimerization. TiO_2 NP aggregation preferentially occurs as a result of the low coverage of MV^{2+} units on the surface of the NPs (Figure S8a) and because of inter-particle interactions caused by the short length of the linker between the MV^{2+} and the catechol. TEM images showed that the TiO_2 NPs aggregated to form micrometer-sized assemblies from the original well-dispersed nanometer-sized particles (Figure 2a,b). These results were consistent with those obtained from dynamic light scattering (DLS) experiments and confirmed what was observed visually. From optical measurements (DLS and UV/Vis absorption spectroscopy; Figures S13, 15), it was also found that the concentration of CB[8] had a significant impact on the degree and rate of aggregation. Considering the measured redox waves in the cyclic voltammograms attributed to the $2(MV^{+\bullet})$@CB[8] complex (Figure S8b), CB[8] played an important role in promoting the dimerization of the

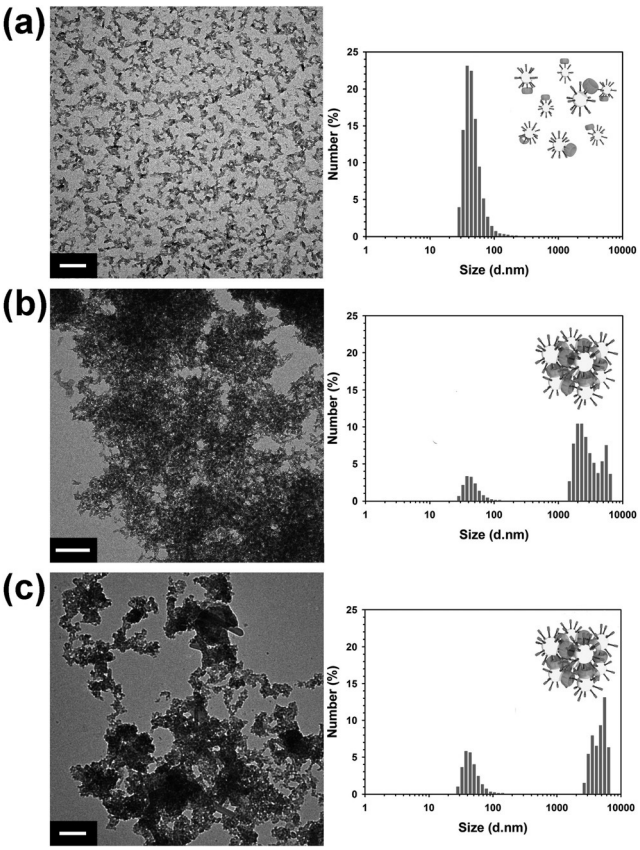

Figure 2. TEM images and DLS results of MV^{2+}–TiO_2 NPs in solution in water a) before self-assembly, and b) after self-assembly induced by chemical reduction or c) photochemical reduction processes. Scale bars = 200 nm.

$MV^{+\bullet}$ radical cation. On the other hand, the photochemical reduction of the MV^{2+}–TiO_2 NPs can be realized in the presence of CB[8] as the host and isopropanol as the hole scavenger. The mixture was saturated with argon gas by bubbling for at least 30 minutes. After exposure to UV light ($\lambda = 365$ nm) for 20 minutes, the transparent solution turned opaque and precipitation occurred (Figures S10, S11, and S14). Interestingly, in contrast to the chemical reduction method, no remarkable color change was observed, which was as a result of the incomplete photoreduction of MV^{2+} to $MV^{+\bullet}$ (Figure S10d). However, the incomplete photoreduction does not affect the aggregation of TiO_2 NPs, as demonstrated by similar TEM spectra and DLS data (Figure 2c) for the system assembled both by photochemical and chemical reduction methods. However, control experiments (Table S1) have shown that in the absence of CB[8], radical cation dimerization of $MV^{+\bullet}$ occurs and visually there is no evidence of NP aggregation. According to the report of Kim et al.,[6a] the CB[8]-enhanced dimerization constant of $MV^{+\bullet}$ in water was 2×10^7 M^{-1}, almost 10^5 times larger than that for the dimerization of the $MV^{+\bullet}$ radical cation without CB[8] in aqueous solution. Considering the similar behavior on the surface of this CB[8]-enhanced host–guest system, it could be stated that the CB[8]-enhanced recognition was significant in the system of photo-controlled mode.

UV/Vis absorption spectra were recorded to confirm that radical cation dimerization had occurred in response to chemical or photochemical stimuli. As shown in Figure S16a, a characteristic strong absorption band in the UV region was measured for the MV^{2+}–TiO_2 solution attributable to TiO_2 NPs.[10a,11] The weaker absorption features in the visible region can be ascribed to the surface complexation of the particles by enediol ligands.[10a,c] In the case of the chemical reduction process, a remarkable red-shift of the major absorption band from $\lambda = 320$ nm (before reduction) to 370 nm (after reduction) can be detected (Figure S16b). This red-shift can be explained by a change in the sizes of the TiO_2 NPs caused by aggregation after addition of $Na_2S_2O_4$, as a result of the quantum size effect.[13] The spectrum shown in Figure S16c, obtained by removing the background absorbance of MV^{2+}–TiO_2 solutions, exhibited bands at $\lambda = 400$ nm and 600 nm. These absorption bands have been shown to be characteristic of $MV^{+\bullet}$ dimerization in the cavity of CB[8],[6a] indicating the formation of the $MV^{+\bullet}$ radical cation.

To further demonstrate the formation of the $MV^{+\bullet}$ radical cation in response to chemical and photochemical stimuli, electron paramagnetic resonance (EPR) measurements was conducted (Figure S16d–g). In both cases, EPR signals for the $MV^{+\bullet}$ radical cation were clearly detected.[7a] To obtain greater insight into the electronic structure of the paramagnetic species, the *g* value was determined by measuring the field and the frequency at which resonance occurs. A *g* value of 2.0063 was recorded for the system, which was very close to that of the free electron of the $MV^{+\bullet}$ unit.[14] After addition of excess H_2O_2 as the oxidant to convert the $MV^{+\bullet}$ radical cations back into MV^{2+} dications, no radical was detected by EPR. Conversion of $MV^{+\bullet}$ radical cations back into MV^{2+} dications was accompanied by disassembly of the assembled NPs back into the original dispersed state without any obvious remaining aggregation (Figure S12), indicating that this system is reversible. It should be noted that in the case of photochemical reduction, the inverse process can be also driven by stirring and exposure to molecular oxygen, where oxygen will quench the $MV^{+\bullet}$ radical cations. Thus, the reversible photochemical reduction process can be considered to be "clean" as it uses light irradiation and oxygen as the fuels, rendering it potentially useful for practical application.

To obtain a greater understanding of the mechanism of the photoinduced assembly process, several control experiments were undertaken (Figure S13, Table S1). On the basis of these experiments, it was found that three conditions are necessary to achieve photoinduced assembly: 1) isopropanol should be present as a hole scavenger to remove the photoexcited holes on the valence band (VB) of TiO_2;[8e] 2) the dissolved oxygen in the solution should be removed; 3) the system should be kept at around pH 7 because of the pH-dependent redox potential of the conduction band (CB) of TiO_2, ensuring photoexcited electron transfer to the MV^{2+} unit.[8a] Considering these conditions, we propose a possible mechanism (Figure 3a) for photocontrolled assembly of MV^{2+}–TiO_2 NPs. First, upon irradiation with UV light, electrons were excited to the conduction band of TiO_2, leaving the same number of holes in the valence band. In neutral solution, the redox potential of the conduction band of TiO_2 was higher than that of $MV^{+\bullet}/MV^{2+}$. The electron on the conduction band can transfer to MV^{2+} through the enediol covalent linker, forming the $MV^{+\bullet}$ radical cation, where the enediol linker ensured a high efficiency of electron transfer (ET). As a result of the lack of dissolved oxygen, the $MV^{+\bullet}$ radical cation formed can dimerize within the cavity of CB[8], leading to the assembly of the TiO_2 NPs. At the same time, the presence of isopropanol can remove the holes formed upon light irradiation, rendering the photoreduction process continuous.[8e]

Switchable catalysts whose activity can be switched by an external stimulus have attracted scientists[15] because of their

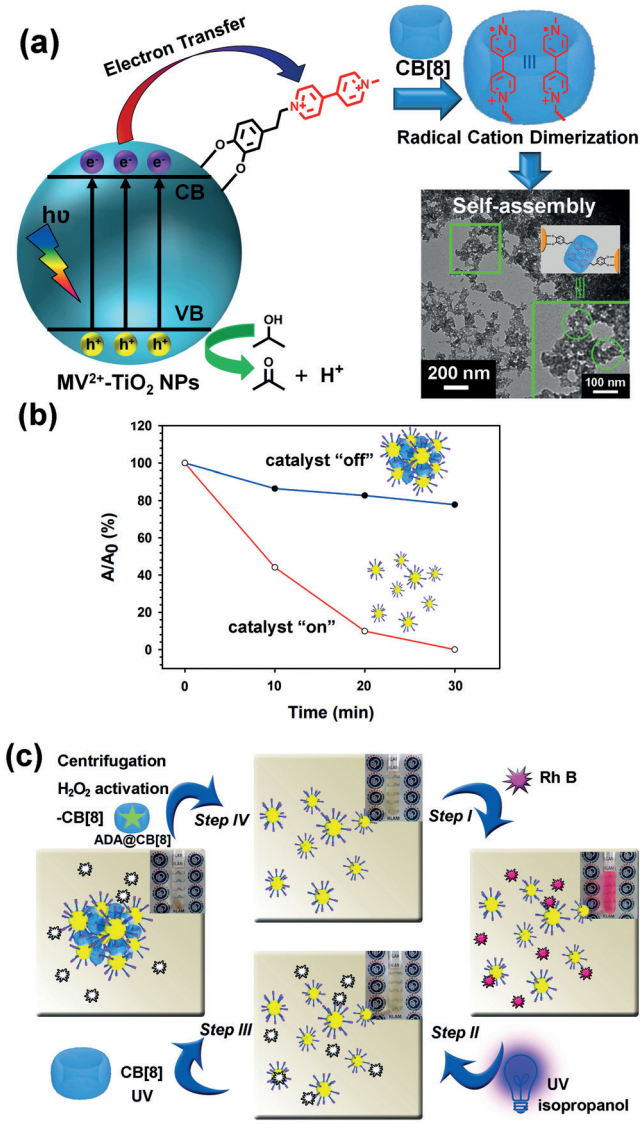

Figure 3. a) The mechanism of photocontrolled assembly of MV^{2+}–TiO_2 NPs by CB[8]-enhanced radical cation dimerization interactions. b) RhB decolorization curves (A = absorption intensity) where the process is catalyzed by disassembled MV^{2+}–TiO_2 NPs (catalyst "on") and the assembled MV^{2+}–TiO_2 precipitate (catalyst "off"). c) Schematic representation showing recycling of the MV^{2+}–TiO_2 photocatalysts by means of a "clean" photoreduction-induced aggregation method.

promising application in organic synthesis and even in biological fields. The controllable self-assembly behavior of MV^{2+}–TiO_2 NPs in response to two types of stimuli can be used to develop switchable photocatalysis. Rhodamine B (RhB), with a typical absorption band around $\lambda = 550$ nm, was selected as the dye substrate.[11] After degassing a mixture of RhB, MV^{2+}–TiO_2, and isopropanol (in the absence of CB[8]) with Ar gas for 30 minutes, the mixture was exposed to UV light ($\lambda = 365$ nm). The dispersed state of MV^{2+}–TiO_2 showed an efficient RhB decolorization ability, which relied on the fact that the produced electrons efficiently converted RhB into leuco RhB (LRhB) in 30 minutes (representing the "on" state of the catalyst; Figure 3b). In contrast, the aggregated TiO_2 NPs generated by photochemical reduction exhibited remarkably different photocatalytic activity for the decolorization of RhB (Figure 3b). In this case, the degree of decolorization was less than 20%, representing the "off" state of catalyst. The remarkable difference in photocatalytic activity in the two cases can be explained to be as a result of the decreased specific surface area after TiO_2 NP aggregation by CB[8]-enhanced radical cation dimerization.

Recycling of TiO_2 catalysts, especially water-soluble TiO_2 catalysts, has proven to be a major challenge.[16] The reversible assembly of nanosized MV^{2+}–TiO_2 NPs into larger microsized particles was expected to provide a new method to recycle TiO_2 NPs. As shown in Figure 3c, a recycling process for the MV^{2+}–TiO_2 catalysts, which had been used for decolorization of the RhB dye, was performed in a quartz tube. First, the RhB dye was added into an aqueous solution of MV^{2+}–TiO_2 NPs (Figure 3c, step I). After complete decolorization in the presence of excess isopropanol upon irradiation with UV light ($\lambda = 365$ nm; step II), CB[8] was added into the solution of MV^{2+}–TiO_2 NPs. UV irradiation for 20 minutes resulted in the aggregation of the TiO_2 NPs to form a precipitate (Figure 3c; step III). Centrifugation was used to separate the precipitate and the catalysts were activated by treatment with a solution of excess H_2O_2. CB[8] could be then removed by addition of excess 1-adamantanamine hydrochloride (ADA)[17] and $Na_2S_2O_4$ followed by centrifugation (step IV; see the Supporting Information). In fact, this reversible supramolecular method changed the water solubility of the TiO_2 NPs and could be used to successfully recycle the catalyst.

In summary, we have demonstrated that the self-assembly of TiO_2 NPs functionalized with methyl viologen is reversible and can be controlled either chemically or photochemically through a CB[8]-enhanced radical cation dimerization process. Interestingly, the consequent dual-stimuli-responsive self-assembly can switch the photocatalytic activity of MV^{2+}–TiO_2 NPs. Additionally, the reversible supramolecular method to aggregate water-soluble NPs can be used to easily recycle catalysts. The combination of semiconductor NPs and supramolecular interactions could provide new means to construct more complicated hybrid materials.

Acknowledgements

We thank the NSFC/China (21421004, 21272073, and 21190033) and the National Basic Research 973 Program for financial support. D.H.Q. thanks the Fok Ying Tong Education Foundation (121069), the Fundamental Research Funds for the Central Universities, and the Innovation Program of Shanghai Municipal Education Commission for financial support. We are grateful to the referees for their helpful and valuable comments.

Keywords: methyl viologen · nanoparticles · self-assembly · stimuli-responsive materials · titanium

How to cite: *Angew. Chem. Int. Ed.* **2015**, *54*, 15789–15793
Angew. Chem. **2015**, *127*, 16015–16019

[1] a) V. Balzani, M. Venturi, A. Credi, *Molecular Devices and Machines. Concepts and Perspectives for the Nanoworld*, 2nd ed., Wiley-VCH, Weinheim, **2008**; b) L. Yang, X. Tan, Z. Wang, X. Zhang, *Chem. Rev.* **2015**, *115*, 7196–7239; c) D. H. Qu, Q. C. Wang, Q. W. Zhang, X. Ma, H. Tian, *Chem. Rev.* **2015**, *115*, 7543–7588; d) M. Xue, Y. Yang, X. Chi, X. Yan, F. Huang, *Chem. Rev.* **2015**, *115*, 7398–7501; e) G. Ragazzon, M. Baroncini, S. Silvi, M. Venturi, A. Credi, *Nat. Nanotechnol.* **2015**, *10*, 70–75; f) H. L. Sun, Y. Chen, J. Zhao, Y. Liu, *Angew. Chem. Int. Ed.* **2015**, *54*, 9376–9380; *Angew. Chem.* **2015**, *127*, 9508–9512; g) C. Stoffelen, J. Voskuhl, P. Jonkheijm, J. Huskens, *Angew. Chem. Int. Ed.* **2014**, *53*, 3400–3404; *Angew. Chem.* **2014**, *126*, 3468–3472; h) G. Gröger, W. Meyer-Zaika, C. Böttcher, F. Gröhn, C. Ruthard, C. Schmuck, *J. Am. Chem. Soc.* **2011**, *133*, 8961–8971; i) T. Heinrich, C. H. H. Traulsen, M. Holzweber, S. Richter, V. Kunz, S. K. Kastner, S. O. Krabbenborg, J. Huskens, W. E. S. Unger, C. A. Schalley, *J. Am. Chem. Soc.* **2015**, *137*, 4382–4390.

[2] a) A. C. Fahrenbach, S. C. Warren, J. T. Incorvati, A. J. Avestro, J. C. Barnes, J. F. Stoddart, B. A. Grzybowski, *Adv. Mater.* **2013**, *25*, 331–348; b) Y. W. Yang, Y. L. Sun, N. Song, *Acc. Chem. Res.* **2014**, *47*, 1950–1960; c) A. B. Descalzo, R. Martínez-Máñez, F. Sancenón, K. Hoffmann, K. Rurack, *Angew. Chem. Int. Ed.* **2006**, *45*, 5924–5948; *Angew. Chem.* **2006**, *118*, 6068–6093; d) R. Klajn, J. F. Stoddart, B. A. Grzybowski, *Chem. Soc. Rev.* **2010**, *39*, 2203–2237; e) H. J. Kim, M. H. Lee, L. Mutihac, J. Vicens, J. S. Kim, *Chem. Soc. Rev.* **2012**, *41*, 1173–1190; f) B. K. Pathem, S. A. Claridge, Y. B. Zheng, P. S. Weiss, *Annu. Rev. Phys. Chem.* **2013**, *64*, 605–630; g) H. Yang, B. Yuan, X. Zhang, O. A. Scherman, *Acc. Chem. Res.* **2014**, *47*, 2106–2115; h) S. Silvi, M. Venturi, A. Credi, *J. Mater. Chem.* **2009**, *19*, 2279–2294; i) V. Balzani, A. Credi, M. Venturi, *ChemPhysChem* **2008**, *9*, 202–220.

[3] a) D. Manna, T. Udayabhaskararao, H. Zhao, R. Klajn, *Angew. Chem. Int. Ed.* **2015**, *54*, 12394–12397; *Angew. Chem.* **2015**, *127*, 12571–12574; b) H. Li, D. X. Chen, Y. L. Sun, Y. B. Zheng, L. L. Tan, P. S. Weiss, Y. W. Yang, *J. Am. Chem. Soc.* **2013**, *135*, 1570–1576; c) G. Yu, M. Xue, Z. Zhang, J. Li, C. Han, F. Huang, *J. Am. Chem. Soc.* **2012**, *134*, 13248–13251; d) J. P. Coelho, G. G. Rubio, A. Delices, J. O. Barcina, C. Salgado, D. Ávila, O. P. Rodríguez, G. Tardajos, A. G. Martínez, *Angew. Chem. Int. Ed.* **2014**, *53*, 12751–12755; *Angew. Chem.* **2014**, *126*, 12965–12969; e) S. Sankaran, M. C. Kiren, P. Jonkheijm, *ACS Nano* **2015**, *9*, 3579–3586.

[4] a) R. Klajn, M. A. Olson, P. J. Wesson, L. Fang, A. Coskun, A. Trabolso, S. Soh, J. F. Stoddart, B. A. Grzybowski, *Nat. Chem.* **2009**, *1*, 733–738; b) Y. Lan, Y. C. Wu, A. Karas, O. A. Scherman, *Angew. Chem. Int. Ed.* **2014**, *53*, 2166–2169; *Angew. Chem.*

2014, *126*, 2198 – 2201; c) J. A. Krings, B. Vonhören, P. Tegeder, V. Siozios, M. Peterlechner, B. J. Ravoo, *J. Mater. Chem. A* **2014**, *2*, 9587 – 9593; d) P. Taladriz-Blanco, N. J. Buurma, L. Rodriguez-Lorenzo, J. Pérez-Juste, L. M. Liz-Marzán, P. Hervés, *J. Mater. Chem.* **2011**, *21*, 16880 – 16887; e) L. L. Zhu, H. Yan, C. Y. Ang, K. T. Nguyen, M. H. Li, Y. L. Zhao, *Chem. Eur. J.* **2012**, *18*, 13979 – 13983; f) N. M. Dimitrijevic, Z. V. Saponjic, B. M. Rabatic, T. Rajh, *J. Am. Chem. Soc.* **2005**, *127*, 1344 – 1345; g) C. Yang, Z. Yang, H. Gu, C. K. Chang, P. Chao, B. Xu, *Chem. Mater.* **2008**, *20*, 7514 – 7520; h) R. J. Coulston, S. T. Jones, T. C. Lee, E. A. Appel, O. A. Scherman, *Chem. Commun.* **2011**, *47*, 164 – 166.

[5] a) Y. Shiraishi, E. Shirakawa, K. Tanaka, H. Sakamoto, S. Ichikawa, T. Hirai, *ACS Appl. Mater. Interfaces* **2014**, *6*, 7554 – 7562; b) S. Das, P. Ranjan, P. S. Maiti, G. Singh, G. Leitus, R. Klajn, *Adv. Mater.* **2013**, *25*, 422 – 426; c) R. W. Taylor, T. C. Lee, O. A. Scherman, R. Esteban, J. Aizpurua, F. M. Huang, J. J. Baumberg, S. Mahajan, *ACS Nano* **2011**, *5*, 3878 – 3887; d) J. W. Lee, R. Klajn, *Chem. Commun.* **2015**, *51*, 2036 – 2039; e) A. Aydogan, G. Lee, C. H. Lee, J. L. Sessler, *Chem. Eur. J.* **2015**, *21*, 2368 – 2376; f) O. Chovnik, R. Balgley, J. R. Goldman, R. Klajn, *J. Am. Chem. Soc.* **2012**, *134*, 19564 – 19567; g) Y. Yao, Y. Wang, F. Huang, *Chem. Sci.* **2014**, *5*, 4312 – 4316; h) H. Han, J. Y. Lee, X. Lu, *Chem. Commun.* **2013**, *49*, 6122 – 6124; i) S. Chen, C. X. Guo, Q. Zhao, X. Lu, *Chem. Eur. J.* **2014**, *20*, 14057 – 14062.

[6] a) W. S. Jeon, H. J. Kim, C. Lee, K. Kim, *Chem. Commun.* **2002**, 1828 – 1829; b) W. S. Jeon, A. Y. Ziganshina, J. W. Lee, Y. H. Ko, J. K. Kang, C. Lee, K. Kim, *Angew. Chem. Int. Ed.* **2003**, *42*, 4097 – 4100; *Angew. Chem.* **2003**, *115*, 4231 – 4234; c) J. W. Lee, S. Samal, N. Selvapalam, H. J. Kim, K. Kim, *Acc. Chem. Res.* **2003**, *36*, 621 – 630; d) Y. H. Ko, E. Kim, I. Hwang, K. Kim, *Chem. Commun.* **2007**, 1305 – 1315.

[7] a) A. Trabolsi, N. Khashab, A. C. Fahrenbach, D. C. Friedman, M. T. Colvin, K. K. Coti, D. Benitez, E. Tkatchouk, J. C. Olsen, M. Belowich, R. Carmielli, H. A. Khatib, W. A. Goddard, M. R. Wasielewski, J. F. Stoddart, *Nat. Chem.* **2010**, *2*, 42 – 49; b) H. Li, A. C. Fahrenbach, A. Coskun, Z. Zhu, G. Barin, Y. L. Zhao, Y. Botros, J. P. Sauvage, J. F. Stoddart, *Angew. Chem. Int. Ed.* **2011**, *50*, 6782 – 6788; *Angew. Chem.* **2011**, *123*, 6914 – 6920; c) D. H. Qu, H. Tian, *Chem. Sci.* **2011**, *2*, 1011 – 1015.

[8] a) J. Moser, M. Grätzel, *J. Am. Chem. Soc.* **1983**, *105*, 6547 – 6555; b) M. Grätzel, J. Moser, *Proc. Natl. Acad. Sci. USA* **1983**, *80*, 3129 – 3132; c) M. D. Ward, J. R. White, A. J. Bard, *J. Am. Chem. Soc.* **1983**, *105*, 27 – 31; d) T. Tachikawa, S. Tojo, M. Fujitsuka, T. Majima, *Langmuir* **2004**, *20*, 9441 – 9444; e) I. Willner, Y. Eichen, *J. Am. Chem. Soc.* **1987**, *109*, 6862 – 6863.

[9] a) S. Wang, R. Gao, F. Zhou, M. Selke, *J. Mater. Chem.* **2004**, *14*, 487 – 493; b) Y. Shiraishi, Y. Sugano, S. Tanaka, T. Hirai, *Angew. Chem. Int. Ed.* **2010**, *49*, 1656 – 1660; *Angew. Chem.* **2010**, *122*, 1700 – 1704; c) D. Tsukamoto, Y. Shiraishi, Y. Sugano, S. Ichikawa, S. Tanaka, T. Hirai, *J. Am. Chem. Soc.* **2012**, *134*, 6309 – 6315.

[10] a) M. Niederberger, G. Garnweitner, F. Krumeich, R. Nesper, H. Cölfen, M. Antonietti, *Chem. Mater.* **2004**, *16*, 1202 – 1208; b) I. A. Janković, Z. V. Šaponjić, M. I. Čomor, J. M. Nedeljković, *J. Phys. Chem. C* **2009**, *113*, 12645 – 12652; c) T. Rajh, L. X. Chen, K. Lukas, T. Liu, M. C. Thurnauer, D. M. Tiede, *J. Phys. Chem. B* **2002**, *106*, 10543 – 10552; d) T. Kotsokechagia, F. Cellesi, A. Thomas, M. Niederberger, N. Tirelli, *Langmuir* **2008**, *24*, 6988 – 6997.

[11] W. Wang, M. Ye, L. He, Y. Yin, *Nano Lett.* **2014**, *14*, 1681 – 1686.

[12] a) L. X. Chen, T. Rajh, Z. Wang, M. C. Thurnauer, *J. Phys. Chem. B* **1997**, *101*, 10688 – 10697; b) S. W. Chen, K. Huang, *J. Cluster Sci.* **2000**, *11*, 405 – 422; c) N. Nakamura, H. X. Huang, D. J. Qian, J. Miyake, *Langmuir* **2002**, *18*, 5804 – 5809.

[13] a) C. Kormann, D. W. Bahnemann, M. R. Hoffmann, *J. Phys. Chem.* **1988**, *92*, 5196 – 5201; b) N. Serpone, D. Lawless, R. Khairutdinov, *J. Phys. Chem.* **1995**, *99*, 16646 – 16654.

[14] J. C. S. Johnson, H. S. Gutowsky, *J. Chem. Phys.* **1963**, *39*, 58 – 62.

[15] a) V. Blanco, D. A. Leigh, V. Marcos, *Chem. Soc. Rev.* **2015**, *44*, 5341 – 5370; b) V. Blanco, A. Carlone, K. D. Hänni, D. A. Leigh, B. Lewandowski, *Angew. Chem. Int. Ed.* **2012**, *51*, 5166 – 5169; *Angew. Chem.* **2012**, *124*, 5256 – 5259; c) S. De, S. Pramanik, M. Schmittel, *Angew. Chem. Int. Ed.* **2014**, *53*, 14255 – 14259; *Angew. Chem.* **2014**, *126*, 14480 – 14484; d) M. Schmittel, S. Pramanik, S. De, *Chem. Commun.* **2012**, *48*, 11730 – 11732; e) J. B. Wang, B. L. Feringa, *Science* **2011**, *331*, 1429 – 1432.

[16] a) C. F. Zhang, L. G. Qiu, F. Ke, Y. J. Zhu, Y. P. Yuan, G. S. Xu, X. Jiang, *J. Mater. Chem. A* **2013**, *1*, 14329 – 14334; b) D. H. Xia, T. W. Ng, T. C. An, G. Y. Li, Y. Li, H. Y. Yip, H. J. Zhao, A. H. Lu, P. K. Wong, *Environ. Sci. Technol.* **2013**, *47*, 11166 – 11173.

[17] a) Y. Lan, X. J. Loh, J. Geng, Z. Walsh, O. A. Scherman, *Chem. Commun.* **2012**, *48*, 8757 – 8759; b) U. Rauwald, J. del Barrio, X. J. Loh, O. A. Scherman, *Chem. Commun.* **2011**, *47*, 6000 – 6002.

Received: September 28, 2015
Revised: October 15, 2015
Published online: November 5, 2015

